Neurophysiology of a VLSI spiking neural network: LANN21

Stefano Fusi[*]
INFN, Sezione Roma I
Università di Roma "La Sapienza"
Pza Aldo Moro 2, I-00185, Roma
fusi@jupiter.roma1.infn.it

Paolo Del Giudice[†]
Physics Lab, Istituto Superiore di Sanità
Vle Regina Elena 299, Roma
paolo@ibmteo.iss.infn.it

Daniel J. Amit[‡]
Dipartimento di Fisica
Università di Roma "La Sapienza"
Ple Aldo Moro 2, I-00185, Roma
amit@surete.roma1.infn.it

Abstract

A recurrent network of 21 linear integrate-and-fire (LIF) neurons (14 excitatory; 7 inhibitory) connected by 60 spike-driven, excitatory, plastic synapses and 35 inhibitory synapses is implemented in analog VLSI. The connectivity pattern is random and at a level of 30%. The synaptic efficacies have two stable values as long term memory. Each neuron receives also an external afferent current. We present "neuro-physiological" recordings of the collective characteristics of the network at frozen synaptic efficacies. Examining spike rasters we show that in absence of synaptic couplings and for constant external currents, the neurons spike in a regular fashion. Keeping the excitatory part of the network isolated, as the strength of the synapses rises the neuronal spiking becomes increasingly irregular, as expressed in coefficient of variability (CV) of inter-spike intervals (ISI). The rates are high, in absence of inhibition and are well described by mean-field theory. Inhibition is then turned on, the rates decrease; variability remains and population activity fluctuations appear, as predicted by mean-field theory.

We conclude that the collective behavior of the pilot network produces distributed noise expressed in the ISI distribution, as would be required to control slow stochastic learning, and that the random connectivity acts to make the dynamics of the network noisy even in the absence of noise in the external afferents.

[*]http://jupiter.roma1.infn.it
[†]INFN, Gruppo Collegato Sanità
[‡]INFN, Sezione Roma I

1 The neuron

The implemented LIF (Linear Integrate and Fire) neuron is a modified version of the Mead neuron [1, 2]. The dynamics of the neuron's depolarization V, is given by:

$$\frac{dV}{dt} = -\beta + I(t) \tag{1}$$

where I is the total afferent current and β is a constant loss. These equations are complemented by the constraint that V cannot go below 0, whatever its input.

The neuron linearly integrates the afferent current, with a constant leak β, and emits a spike when $V = \theta$; after τ_0 (=50μs, the width of the spike) V is reset to H. τ_0 plays the role of an absolute refractory period, since, during the emission of the spike, no current is injected in the neuron. In the implementation θ=1.4V; H=0.5V.

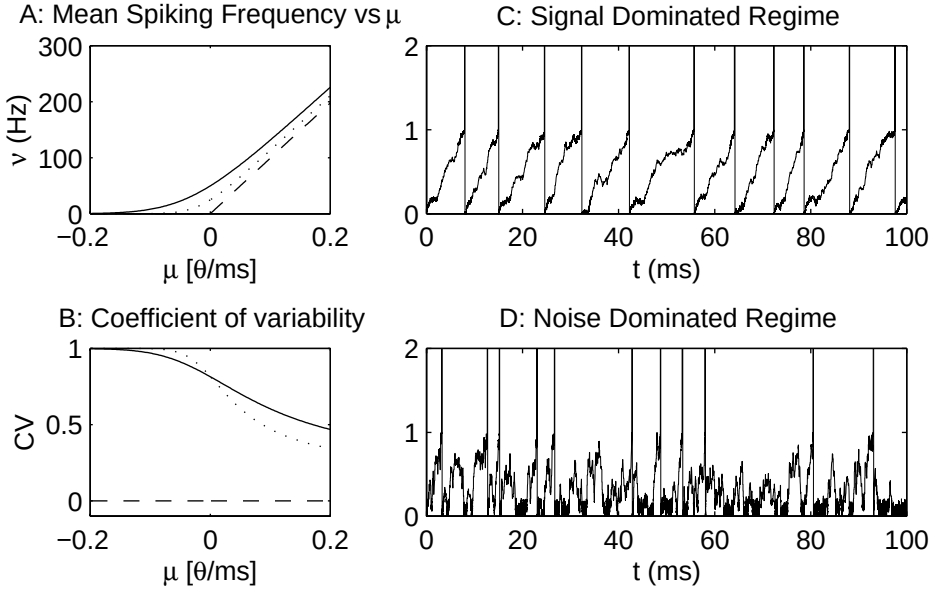

Figure 1: Single neuron response: A: Output rate vs drift ($\mu =< I > -\beta$) for three values of σ (dashed line: $\sigma^2 = 0$, dotted line: $\sigma^2 = 0.025$, solid line: $\sigma^2 = 0.05$ in units of θ^2/ms), theory [3]; B: CV vs μ for the same values of σ^2 as in A; C: Simulation of the evolution of the depolarization (Eq. 1) for Gaussian input current with $\mu = 0.19\ \theta/ms$, $\sigma^2 = 0.011\ \theta^2/ms$. The CV is 0.23. D: simulation for $\mu = -0.096\ \theta/ms$, $\sigma^2 = 0.26\ \theta^2/ms$. CV= 0.85. In both C and D the output rate is $100Hz$, $H = 0$.

Single neuron response to noisy input: When the afferent current I is drawn from a Gaussian distribution with mean $\langle I \rangle$ and variance σ^2, its spike emission rate, $\nu(\mu, \sigma)$, is [3]:

$$\nu = \Phi(\mu, \sigma) = \left[\tau_0 + \frac{\sigma^2}{2\mu^2} \left(e^{\frac{-2\mu\theta}{\sigma^2}} - e^{\frac{-2\mu H}{\sigma^2}} \right) + \frac{\theta - H}{\mu} \right]^{-1}. \tag{2}$$

It is depicted in Fig. 1A vs the drift μ ($\equiv \langle I \rangle - \beta$), for three values of σ. If σ=0, the response is threshold-linear [4] (dashed curve): ν=0 , if $\langle I \rangle \leq \beta$; otherwise

$$\nu = \left(\frac{\theta - H}{\mu} + \tau_0 \right)^{-1}. \tag{3}$$

This would be the expected response if the neurons are decoupled and the afferent current is noiseless. If noise is present in the afferent current, the rate vs the drift becomes concave at low currents and the rate is non-zero even for negative drift. In Fig. 1C,D we show the temporal evolution of the depolarization (simulated) of the implemented neuron for positive and negative drift, and the output frequency of the neuron as a function of the drift, for different values of σ. In Fig. 1B we present the coefficient of variability CV, defined as:

$$CV = \sqrt{< T^2 > - < T >^2} / < T >$$

where $T = 1/\nu$ is the average time between two subsequent spikes emitted by the neuron.

2 The network

The neurons are connected by spike-driven plastic synapses [5] between the excitatory neurons and fixed valued (excitatory-inhibitory, inhibitory-excitatory, inhibitory-inhibitory) synapses. In this report we concentrate on the collective properties of neurons, so all synapses are kept fixed and a detailed description of the synapse is omitted. The connectivity in all directions is random and on average each neuron is connected to 30% of the others.

In Fig.2 (left) the layout of the LANN21 (Learning Attractor Neural Network) is shown; on the right the connectivity scheme and the chip I/O is illustrated.

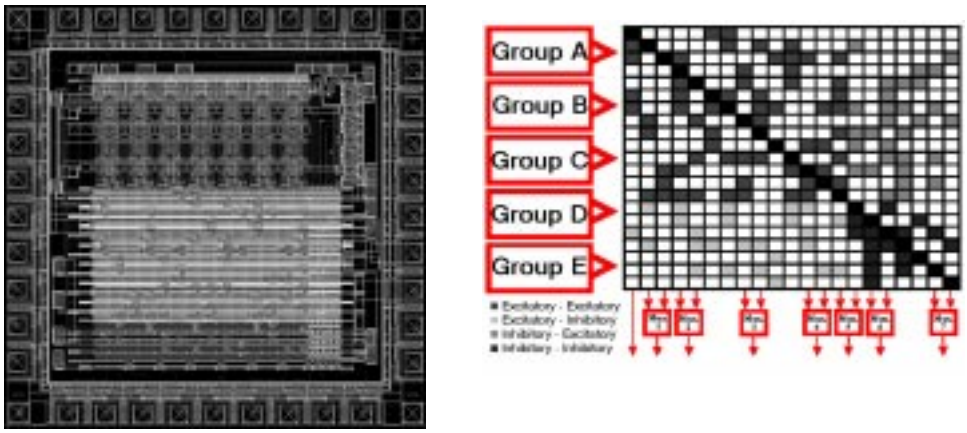

Figure 2: The LANN21 chip: CMOS technology, 1.2μm; the core is 1.5 × 1.38 mm. Left: layout of the chip. In the topmost, central row the 14 excitatory neurons, and the 7 inhibitory neurons are on the righmost column. The scattered patches in the lower part of the chip are the 60 plastic, excitatory-to-excitatory

synapses. The other synapses are barely visible in the lower strip. Right: 4-way connectivity scheme of the network: gray squares are existing synapses; each row represents the "dendritic tree" of one neuron. Black squares indicate that there are no self-interactions. Equal external stimulation current arrives within groups indicated by pointed boxes on the left; spikes can be observed only for neurons with an arrow down (10 excit, 5 inhib), spikes with arrows going out into the same Mux box come out on the same pin and are then de-multiplexed.

Note that when all neurons in the network are excitatory and the stimulating current is constant, the neurons must operate at positive drift, or no spike is emitted and no noise generated.

If the number of neurons is large enough, and the firing probability of each neuron is an independent random variable, the afferent current to each neuron is random, and can be approximated by a Gaussian current [7, 3]. In particular, the average of the current μ and its variance σ^2 can be estimated by:

$$\mu = cJ\nu - \beta + I_{ext} \qquad \sigma^2 = cJ^2\nu$$

where c is the average number afferents, ν is the mean frequency of the afferent neurons, J is the mean strength of the couplings, and I_{ext} is the external afferent current. This is a good approximation even in the case of LANN21, where the number of afferents is rather low.

3 Methods – measuring efficacies

The existing synaptic efficacies are either zero or have another (fixed) value, whose magnitude is externally regulated and is set by a host PC via a programmable micro-processor based board. The actual values of the efficacies must be measured, following their regulation. In LANN21 only the depolarization of one neuron is visible (neuron 0); this neuron has two afferent excitatory synapses, whose efficacy can be directly measured by the jumps induced in the depolarization by pre-synaptic spikes. We have adopted the following procedure to estimate all the synaptic efficacies: 1. All synapses are regulated, the external (constant) currents turned on and spike rates and CVs are measured for all neurons. 2. All synapses are turned off and the resulting rates provide a measurement of afferent mean currents, which are composed of the external currents and the neuron linear decay. Since in absence of interaction, the integration is linear, the mean afferent current μ to each neuron is directly related to its mean spiking frequency ν (see Eq.3):

$$\mu = < I > -\beta = \frac{\nu\theta}{(1 - \nu\tau_0)}$$

The contribution of the external current can be separated from the linear decay by setting $\beta = 0$ and repeating the procedure. 3. Each of the four types of synapses is turned on exclusively and rates and CVs are measured. 4. For each of the four classes the single type of synaptic efficacy involved is varied in MF theory until the computed rates match the measured rates. For example, to determine the inhibitory-excitatory mean efficacy $J_{I\to E}$, all the other couplings are turned off and the average rates are measured. The population of excitatory neurons receive an extra inhibitory current with respect to case 2, and the mean frequency ν_E is lowered. The estimate of $J_{I\to E}$ should satisfy the following self consistency equations:

$$\nu_E = \Phi(\mu_E, \sigma_E)$$

$$\mu_E = I^E_{ext} - \beta_E - c_{I\to E}J_{I\to E}\nu_I, \qquad \sigma^2_E = c_{I\to E}J^2_{I\to E}\nu_I$$

where ν_I and ν_E are the measured average rates of inhibitory and excitatory neurons respectively, $c_{I\to E}$ is the mean number of inhibitory afferents per excitatory neuron, and I^E_{ext} is the mean external afferent current, which has already been determined in step 2.

After all four (average) efficacies are determined this way, MF is applied to the entire network and the rates computed. Those are compared with the rates measured in Step (1). This is a strong consistency check in addition to comparing the excitatory-excitatory efficacy with the one measured directly on neuron 0.

It turns out that when the network does not synchronize the emission rates can be obtained by a MF approach (despite the fact that the number of neurons is rather low).

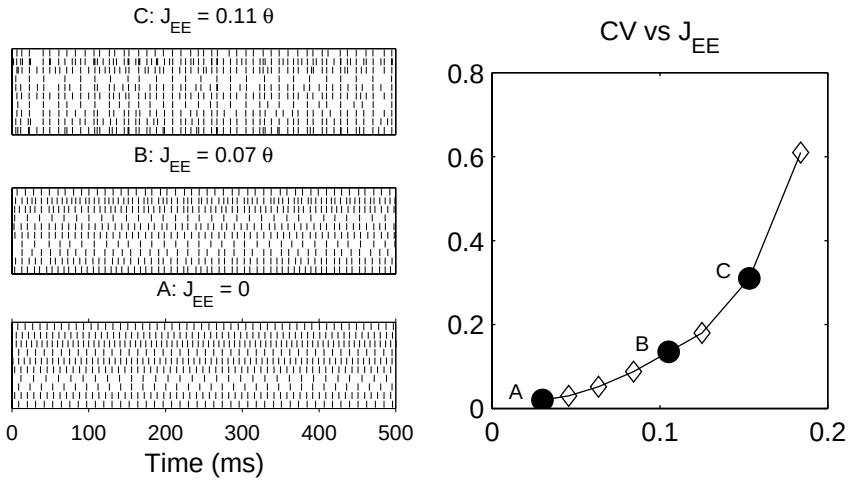

Figure 3: Activity in excitatory network. Left: Spike rasters (0.5 second) for 10 excitatory neurons (no inhibition) for three values of average synaptic efficacy (A:$J = 0$, B:$J = 0.07\theta$, C:$J = 0.11\theta$) in units of the neural threshold (β=0.). Note that spike rates of different neurons are quite different due to the random connectivity in the network which results in a large variability in the number of afferent synapses among neurons. Right: Average CV vs $J_{E\to E}$. The black circles correspond to the rasters sets on the left. Rates are kept constant, as $J_{E\to E}$ varies, by adjusting external currents.

4 Results

4.1 Excitatory network

As synaptic efficacies are turned on, the incoming current to a neuron will include the feedback spikes from other neurons in the network, over and above the (constant) external current. For a disordered system (here due to the random connectivity) spike trains become increasingly irregular. Even though the system is completely deterministic, also on relatively long time scales spike trains cannot be distinguished from noise. (See e.g. [6]). In Fig. 3 (left) we present 0.5 second spike rasters of 10 excitatory neurons of the network (in absence of inhibition) for three values of the average excitatory synaptic efficacy. Fig. 3 (right) presents average CV vs the (measured) synaptic efficacy. The excitatory efficacy is varied holding the average neurons' rate constant, by adjusting the afferent current. CV is increasing with the efficacy as well as with increasing number of afferent synapses. Note that for weak

synapses the neurons emit quite regularly.

For not too high values of the synaptic efficacies (high Js tend to synchronize the neurons' firing and to break the basic hypotheses of the MF approach) we compare observations with the predictions in the MF approximation. We made the comparison for the parameters corresponding to the black points B and C in Fig. 3. For point B, MF: $J_{E\to E} = 95.4$ mV, measured $J_{E\to E}$ is 102 ± 7 mV. For point C, MF: $J_{E\to E} = 138$ mV, measured: 130 ± 21 mV. It is seen that even for such a small network there is good agreement with MF predictions.

4.2 Inhibition included

Turning on the inhibition one can obtain neurons with small negative drift. Inhibition lowers the neuronal drift and hence the rates. This is accompanied by an increase of ISI variability, as measured by CV. It is a consequence of the fact that the neurons move into their noise driven regime, where spikes are emitted due to fluctuations (see e.g. Fig.1D). Fig. 4 presents two sets of raster plots of the 15 visible neurons (5 inhibitory at bottom) for the two sets of couplings in Table 1.

For strong couplings (upper part in Fig. 4), we would have to inject small external currents, to avoid very high level of synchronization in the network; on the other hand, working with very small currents (of the order of nA) is a source of instabilities and needs fine tuning. We therefore inject equal, constant current into excitatory neurons belonging to group A in Fig. 2 (they have common external input), and no current into other neurons. High rates are provoked only in these 4 neurons, which in turn excite the other excitatory neurons as well as the inhibitory ones. In this regime, the neurons exhibit high variability in their spiking times (the average measured CV is 1.06 for the excitatory neurons that do not receive external currents).

A typical weak coupling regime is shown in the lower part of Fig. 4. After estimating the couplings following the procedure described in Section 3, the CV is calculated in MF approximation. The measured average CV of all excitatory neurons is 0.35, the MF prediction is 0.38 (for inhibitory neurons, measured CV: 0.13, MF: 0.14). For the $J_{E\to E}$ coupling, we could compare the MF estimate with the direct measurement of the induced jumps in the depolarization of neuron 0; MF: 0.134 θ, measured: 0.135 θ. The measured average rates are: $\nu_E = 139Hz$ and $\nu_I = 199Hz$; the MF predictions are $\nu_E = 134Hz$ and $\nu_I = 199Hz$.

Network couplings				
	$J_{E\to E}$	$J_{I\to E}$	$J_{E\to I}$	$J_{I\to I}$
Strong couplings	0.235	0.168	0.14	0.06
Weak couplings	0.134	0.084	0.07	0.03

Table 1: Two sets of couplings for the network of Fig. 4. The values (in units of θ) are estimated from MF as described in Section 3.

We conclude that the dynamics of the connected network generates (effective) noise even in absence of noise in the afferent current and this noise can underpin slow stochastic learning [5].

Acknowledgments

We acknowledge the sopport of INFN through the NALS initiative. D. Badoni, A. Salamon and V. Dante designed the chip and the data acquisition system; we thank them for their support during the present work.

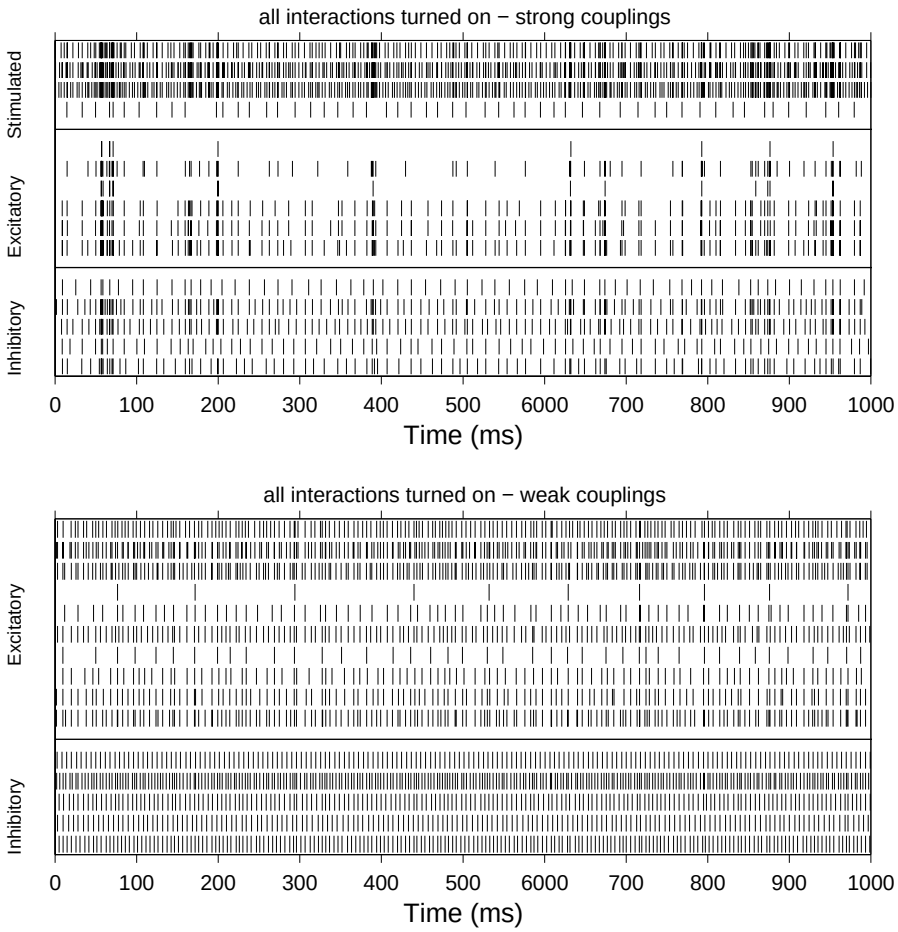

Figure 4: Network with inhibitory neurons: 2 raster sets for 2 sets of synaptic parameters (see Table 1). Only the 4 neurons corresponding to the 4 topmost rows receive external current (equal and constant).

References

[1] Mead C. (1989) *Analog VLSI and Neural System*, Reading, MA: Addison-Wesley

[2] Badoni D., Salamon. A., Salina A., Fusi S., (1999) aVLSI implementation of a learning network with stochastic spike-driven synapse, in preparation

[3] Fusi S. and Mattia M. (1999) Collective behavior of networks with linear (VLSI) integrate-and-fire neurons, *Neural Computation* **11**, 643

[4] Gerstein G.L. and Mandelbrot B. (1964) Random walk models for the spike activity of a single neuron, *Biophysical Journal* **4** 41

[5] Fusi S., Annunziato M., Badoni D., Salamon A. and Amit D.J., (1999) Spike-driven synaptic plasticity: theory, simulation, VLSI implementation, *Neural Computation* (submitted, URL:jupiter.roma1.infn.it)

[6] van Vreeswijk CA, and Sompolinsky H (1996), Chaos in neural networks with balanced excitatory and inhibitory activity *Science*, **274** 1724

[7] Amit D.J. and Brunel N. (1997) Model of global spontaneous activity and local structured activity during delay periods in the cerebral cortex, *Cerebral Cortex* **7** 237